

Paper Review

**GPU-Based Real-Time Approximation of the Ablation Zone for  
Radiofrequency Ablation**

EN 601.456 Computer Integrated Surgery II

CIS II Project 14: Needle Localization In CT-Guided Tumor Ablation

Giang Hoang

[giang@jhu.edu](mailto:giang@jhu.edu)

## CIS II Project Summary

This project aims to develop an algorithm to localize and identify the orientation of the ablation needle in CT images to predict the ablation zone during minimally-invasive tumor ablation procedures. The two phases of the project include: developing a 3D-segmentation algorithm of ablation needles and generating a real-time approximation of the ablation zone.

## Medical Background

### 1. Radiofrequency Ablation Overview

Radiofrequency Ablation is a minimally invasive surgical procedure that utilizes the heat generated from electrical energy to destroy cancer cells (*Wood et al.*). Tumor ablation involves inserting an ablation needle containing radiofrequency electrodes into the tumor site. These electrodes stimulate a high-frequency electric field, which heats up a targeted area in the tumor and induces coagulative necrosis. The efficacy of the treatment is affected by the impedance and heat regulation of the tissue and blood vessels and most importantly, the placement of the ablation needles with respect to the tumor.

### 2. Challenges of Ablation Zone Approximation

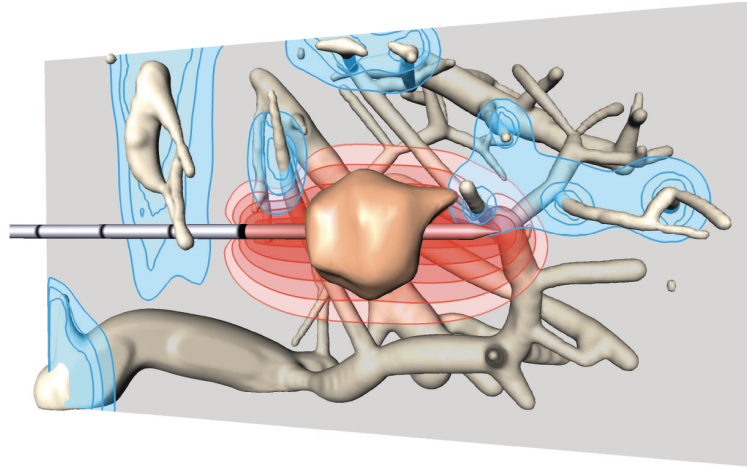
The ablation zone can be approximated from the location and the technical specification of the ablation needle. However, there are additional factors that greatly impact the resulting coagulation effect of the ablation procedure, including the tissue thermal and electrical properties (specific heat, thermal and electrical conductivity) and heatsink effects caused by vessel occlusion (*Wood et al.*). Thus, the ablation treatment plan is very patient-specific and an accurate approximation of the ablation is extremely complex, if not impossible. Moreover, even when the ablation planning is accurate, there is always some mismatch between preoperative and intraoperative conditions, affecting the optimal placement of ablation electrodes. The combination with other procedures, such as hydrodisplacement (fluid instillation) to protect critical structures during ablation, can greatly affect the location planning and the thermal/electrical conductivity of the ablation zone.

## Paper Selection

C. Rieder, T. Kröger, C. Schumann and H. K. Hahn, "GPU-based Real-Time Approximation of the Ablation Zone for Radiofrequency Ablation," in *IEEE Transactions on Visualization and Computer Graphics*, vol. 17, no. 12, pp. 1812-1821, Dec. 2011, doi: 10.1109/TVCG.2011.207.

The paper by Rieder et al. was chosen due to its relevance to the goal of the project. Specifically, the paper presents a novel approach to model the ablation zone while taking into account the heat-sink effects commonly caused by large blood vessels near the tumor

site. The model is developed using complex numerical simulations and graphics hardware, aiming to support the ablation procedure planning process.



## Paper Summary

### 1. Clinical Motivation and Main Points

Multiple studies have shown a high recurrence rate of RFA-treated tumors due to the inaccurate placement of ablation electrodes or the inability to produce a predictable ablation volume. Currently, the ablation zones are typically approximated as ellipsoids surrounding the ablation electrodes specified by the manufacturers. To devise a patient-specific surgical plan, improve ablation accuracy, and lower recurrence rate, a more sophisticated model is required. This study presents a real-time approximation of the estimated ablation zone with respect to the heat-sink effects caused by blood vessels, which aims to support the interactive patient-specific planning of ablation electrode placement in the tumor.

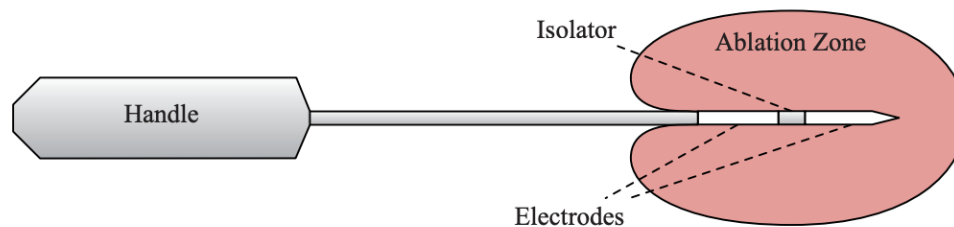


**Fig 1.** Illustration of a bipolar RF applicator with corresponding ablation zone. The two electrodes are separated by an isolator. The applicator shaft is internally cooled resulting in the typical shape of the ablation zone in the direction of the handle. (*Rieder et al.*)

In this paper, the authors proposed a model based on weighted distance fields to approximate the ablation zone, integrated the model into a clinical software assistant, and assessed the model performance by comparing it to other conventional ablation zone approximation methods.

## 2. Mathematical Model

### i. Numerical Simulation Model

The ablation zone approximation is first built based on the numerical simulation described by *Kröger et al.*. This model uses a bio-heat transfer equation to approximate the temperature of tissue at each location within a certain domain of interest surrounding the applicator electrodes.

$$\begin{array}{l}
 \text{Electric conductivity (dependent on T)} \quad \text{Electric potential} \\
 \text{Quasi-static electric potential} \quad \nabla \cdot (\sigma \nabla \phi) = 0 \\
 \\
 \text{Bioheat transfer equation} \quad \rho c \partial_t T - \nabla \cdot (\lambda \nabla T) + v(T - T_{\text{body}}) = q. \\
 \begin{array}{l}
 \text{Density} \quad \text{Specific heat} \quad \text{Thermal conductivity} \quad \text{Relative blood flow rate} \quad \text{Invisible heatsink} \\
 \text{Heat source induced by electric current} \\
 q(x) = \alpha p(x) \\
 p(x) = \sigma |\nabla \phi(x)|^2
 \end{array} \\
 \\
 \text{Initial condition} \quad T(t, \mathbf{x}) = T_{\text{body}} \quad t = 0.
 \end{array}$$

The equations are subjected to multiple boundary conditions listed below.  $\Gamma_{\pm}$  is the boundary of the domain that contains the electrodes,  $\Gamma_{\text{iso}}$  is the boundary of the domain that contains the isoelectric portion, and  $\Gamma_{\text{ves}}$  is the boundary of the domain that contains large blood vessels.

$$\begin{array}{ll}
 \phi(\mathbf{x}) = \pm 1, & \mathbf{x} \in \Gamma_{\pm}, \\
 n(\mathbf{x}) \cdot \nabla \phi(\mathbf{x}) = 0, & \mathbf{x} \in \Gamma_{\text{iso}}, \\
 n(\mathbf{x}) \cdot \nabla \phi(\mathbf{x}) = \frac{n(\mathbf{x}) \cdot (\mathbf{s} - \mathbf{x})}{|\mathbf{s} - \mathbf{x}|^2} \phi(\mathbf{x}), & \mathbf{x} \in \Gamma_{\text{out}}, \\
 T(t, \mathbf{x}) = T_{\text{body}}, & \mathbf{x} \in \Gamma_{\pm} \cup \Gamma_{\text{iso}}, \\
 T(t, \mathbf{x}) = T_{\text{body}}, & \mathbf{x} \in \Gamma_{\text{ves}}, \\
 n(\mathbf{x}) \cdot \nabla T(t, \mathbf{x}) = 0, & \mathbf{x} \in \Gamma_{\text{out}}.
 \end{array}$$

The system is then discretized in both space and time using finite element analysis and backward Euler scheme (*Kröger et al.*). The resulting temperature at a certain location in space and time can be solved and plugged into the equation below to quantify the tissue damage caused by thermal energy generated from the ablation needle. A and E are tissue parameters.

$$D(t, \mathbf{x}) = \int_0^t A \exp\left(\frac{-E}{RT(s, \mathbf{x})}\right) ds.$$

The tissue damage is evaluated throughout the total ablation time ( $t_{\text{max}}$ ) at each location in space. The locations where D surpass the damage threshold to achieve necrosis form the simulated ablation zone:

$$I_{\text{sim}} = \{\mathbf{x} \in \Omega : D(t_{\text{max}}, \mathbf{x}) \geq 1\},$$

## ii. Weighted Distance Field Approximation

Due to the use of finite element analysis, numerical stimulation is extremely time-consuming. Thus, the authors decided to create an approximation of the numerical simulation model using weighted distance field approximation. In other words, the ablation mask  $I_{\text{sim}}$  is approximated by iso-thresholding a weighted distance transform. The weighted distance transform is defined as:

$$\tilde{f}(\mathbf{x}) = \left( \sum_{i=1}^m \sum_{j=1}^n \frac{1}{m \cdot |\mathbf{x} - \mathbf{s}_{ij}|^\alpha} \right)^{-1/\alpha}$$

for  $m$  equals the number of sampling points for each of the  $n$  electrodes. Here, the approximated ablation zone is defined as:

$$I_{\text{zone}}(d, \alpha) = \{\mathbf{x} \in \Omega : f(\mathbf{x}) \leq d\}.$$

where  $d$  is the iso-threshold of  $f(\mathbf{x})$  that represents the size of the ablation zone, and  $\alpha$  is a positive, real parameter that influences the shape of the ablation zone. Specifically, the smaller the value of  $\alpha$ , the more spherical the ablation zone appears. Thus, any ablation zone is now represented by only two parameters:  $\mathbf{d}$  and  $\alpha$ .

To create a lookup database, for any given ablation applicator and given ablation parameters (varying electrode lengths, ablation time, and generator power), optimal values for  $\mathbf{d}$  and  $\alpha$  are solved such that the volumetric difference between  $I_{\text{zone}}$  and  $I_{\text{sim}}$  is minimized. Thus, for every configuration of the ablation tool, one can simply look up the predicted ablation zone in homogenous tissue.

## iii. Modeling the heatsink effects

The thermal equilibrium of the vasculature is approximated using the same bio-heat equation as section (i) without the presence of the applicator as a heat source. The bio-heat equation is then solved in a similar matter to obtain the normalized steady-state temperature  $g(x)$ .

$$g(\mathbf{x}) = 1 - \frac{T(\mathbf{x}) - T_{\text{body}}}{T_{\text{warm}} - T_{\text{body}}} \quad T_{\text{warm}} := T_{\text{body}} + q/\nu$$

The larger the value of  $g(x)$ , the greater the cooling effect.

## iv. Deformation of the ablation zone

By combining the weighted distance transform representing the ablation needle ( $f(x)$ ) and the normalized steady-state temperature of the vasculature ( $g_v(x)$ ), the deformed ablation zone can be generated. The authors also incorporated internal cooling of the ablation needles as a parameter ( $g_a$ ), as it is commonly incorporated into ablation needles to

improve the range of ablation. The optimal transition function for the model was determined to be  $\arcsin()$ .

$$I = \{ \mathbf{x} \in I_{\text{zone}} : \arcsin(\frac{1}{d}f(\mathbf{x})) + \arcsin(g_v(\mathbf{x})) + \arcsin(g_a(\mathbf{x})) \leq \frac{\pi}{2} \}$$

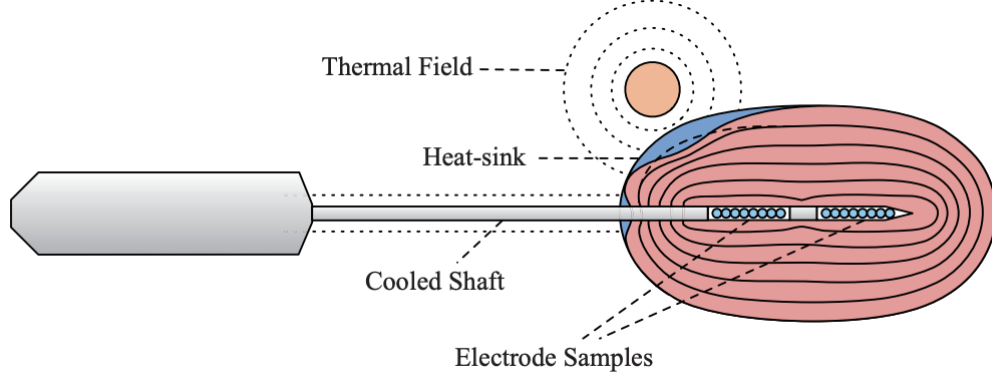


**Fig 2.** Illustration of a complete approximation model for a cooled bipolar applicator and a thermal field of the cooling vasculature (Rieder et al.).

### 3. Technical Application

#### i. Preprocessing

The patient preoperative images are first segmented semi-automatically using a region growing algorithm. Next, the blood vessels are segmented from a region of interest using a Bayesian vessel extraction algorithm. Next, the thermal equilibrium of the vasculature is computed using the equation above for  $g(x)$ .

#### ii. Calculate Ablation Zone

The ablation zone is computed using **Modular Shader Framework**. The algorithm starts with computing the weighted distance field per fragment and then combining it with the cooling effects to form the final approximated ablation zone.

```

input : electrode parameters, thermo field
output: ablation zone mask per fragment

distance ← 0;
for electrode : e ∈ electrodes do
    distance_e ← 0;
    sample_e ← (0,0,0);
    for s ← 0 to electrode samples do
        sample_s ← calcSample(s, params_e);
        dist_s ← distance(sample_e, sample_s);
        distance_e ← distance_e +  $\frac{1}{s_{\max} \text{pow}(dist_s, \alpha)}$ ;
    end
    distance ← distance + distance_e;
end

distance ← pow(distance-1, α-1);
ablationZone ← step(distance, d);
ablationZone ← calcCooling(distance, d, thermoField);

```

## 4. Results

### i. Visualization

The predicted ablation zone is subjected to volume rendering and overlaying on top of a virtual ablation needle. Distance and also multi-parameter contours were also displayed.

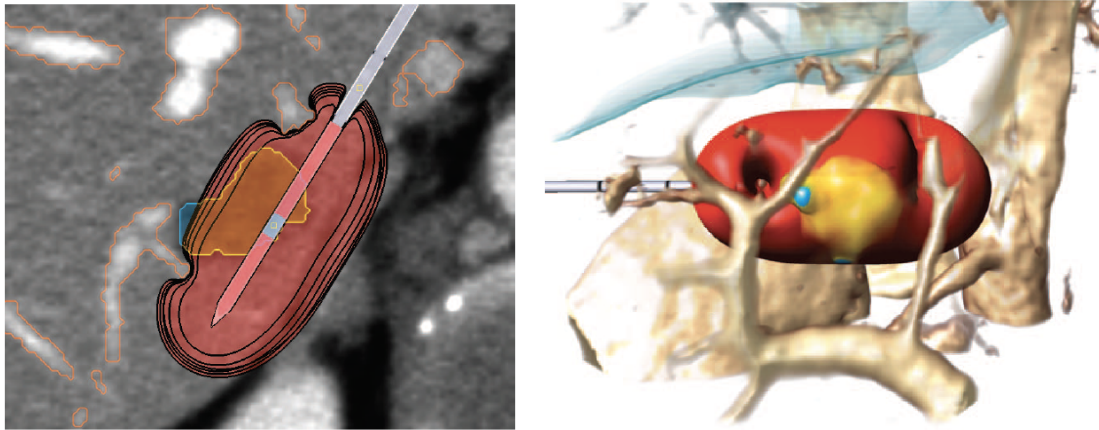


**Fig 3.** (A) Multi-parameter isoline 2D visualization of 1, 2, 4, 8, and 16 minutes of ablation progress. (B) 3D Volume rendered with boundary and silhouette enhancement. (*Rieder et al.*).

### ii. Evaluation

The model is compared to the traditional ellipsoid model and the computationally-intensive numerical simulation model. The resulting ablation zone closely resembles the numerical simulation model and is more realistic than the ellipsoid model. However, the voxel-by-voxel analysis showed no statistical significance between the current model and the ellipsoid model due to the large error associated with the heat-sink model.

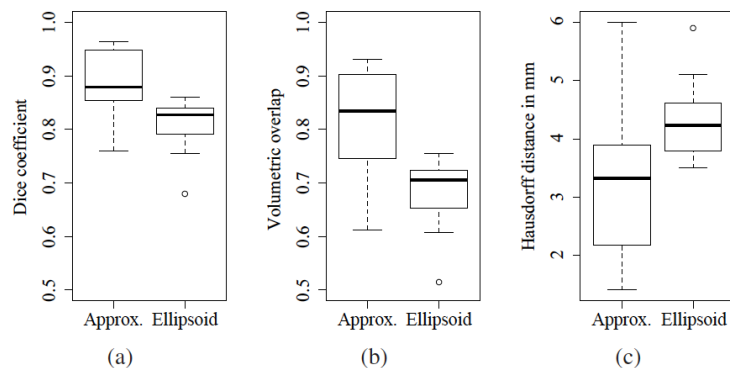


**Fig 4.** The (a) averaged Dice coefficients, (b) averaged volumetric overlap, and (c) Hausdorff distances from 10 simulated masks with the approximation masks and ellipsoid masks. (*Rieder et al.*).

## Critique

### 1. Strengths

The algorithm is very rigorous, detailed, and patient-specific. It successfully models the heatsink effects caused by blood vessels, resulting in a more realistically-looking ablation zone as compared to the traditional ellipsoid model. Especially, the paper was able to generate powerful visualization of the ablation zone, making it a useful model for RFA procedure planning. The ability to visualize multi-parameter contours also makes it easier for interactively planning procedures and can serve as a great asset for medical training.

### 2. Limitations

Due to the rigorous and detailed model, the algorithm is still very computationally intensive. If a patient-specific approach is desired, a whole new database for weighted distance field approximation needs to be made for every patient and every tissue type. The process requires a GPU to run the simulation and can take up to several hours of running time depending on the desired resolution. A lot of inputs, including technical specification and tissue thermal and electrical properties, as well as semiautomatic preprocessing that asks for user inputs are needed to run the algorithm.

Next, the attempt to model the heatsink effects drastically increased the error range of the algorithm, and thus, the difference between the model and the ellipsoid approximation did not achieve statistical significance. This means the stability of the model needs to be improved. Currently, the model can only be used for RFA planning due to its extensive run time. No algorithm to detect and segment real ablation needles has been incorporated to attempt intraoperative navigation.

### 3. Next Steps

As the authors mentioned in the paper, future plans include conducting a user study with medical experts and using real patient data to evaluate the clinical value. The model can also be integrated into an automatic path proposal method for RFA applicator placement. Further studies should also be conducted to improve algorithm efficiency and explore potential for intraoperative application.

## References

- T. Kröger, I. Altrogge, T. Preusser, P. Pereira, D. Schmidt, A. Weihusen, and H. Peitgen. Numerical simulation of radiofrequency ablation with state dependent material parameters in three space dimensions. Proceedings of MICCAI, 4191:380–388, 2006.*
- C. Rieder, T. Kröger, C. Schumann and H. K. Hahn, "GPU-based Real-Time Approximation of the Ablation Zone for Radiofrequency Ablation," in IEEE Transactions on Visualization and Computer Graphics, vol. 17, no. 12, pp. 1812-1821, Dec. 2011, doi: 10.1109/TVCG.2011.207.*
- Wood B.J., Locklin J.K., Viswanathan A, et al. Technologies for guidance of radiofrequency ablation in the multimodality interventional suite of the future. J Vasc Interv Radiol. 2007;18(1 Pt 1):9-24. doi:10.1016/j.jvir.2006.10.013*